JET–P(97)27

Transient Heat Transport Studies Using Laser Ablated Impurity Injection in JET

P Galli[1], A Cherubini, R De Angelis[2], F De Luca[1,3], M Erba[4], R Giannella, G Gorini[1,3], A Jacchia[3], H Jäckel, P Mantica[3], V V Parail, L Porte and A Taroni

JET Joint Undertaking, Abingdon, Oxfordshire, OX14 3EA,

[1]INFM and Physics Department, University of Milano, I-20 133 Milano, Italy.

[2]CRE Frascati, EURATOM-ENEA-CNR Association, I-20 133 Milano, Italy.

[3]Istituto di Fisica del Plasma, EURATOM–CEA Association, I-20 133 Milano, Italy.

[4]EURATOM–CEA Association, C E Cadarache, 13 108 Saint Paul lez Durance, France.

Submitted to Nuclear Fusion

October 1997

ABSTRACT

Following impurity injection by Laser Ablation (LA) in JET plasmas, the electron temperature (T_e) is observed to drop at a rate that cannot be accounted for by changes in radiated power (ΔP_{rad}). T_e starts to drop promptly over a large fraction of the plasma volume which can be explained by a non local change in electron heat diffusivity. The change in diffusivity, $\Delta\chi_e$, is generally short lived, lasting a few milliseconds, even if ΔP_{rad} can persist for longer times. No clear relation between ΔP_{rad} and the strength of the prompt plasma response to LA can be observed, but only those events with $\Delta P_{rad}/P_{rad}>0.5$ give rise to detectable T_e perturbations. The $\Delta\chi_e$ value at the LA time (t_{LA}) is found to increase exponentially with t_{LA} in Hot Ion H mode plasmas reaching values that are much larger than typical Ohmic and H mode levels (for which $\Delta\chi_e \approx 1$ m^2/s). The $\Delta\chi_e$ profile is strongly non uniform in Hot Ion H mode plasmas; moreover, also examples of non monotonic $\Delta\chi_e$ profiles are found in low power plasmas. Energy transport models combining local and non local (or strongly non linear) features are possible candidates for an explanation of these observations.

1. INTRODUCTION

Understanding energy transport in tokamaks remains one of the main challenges in plasma physics research. While the microscopic processes that govern tokamak transport have yet to be identified with confidence, continuous progress is being made in assessing the phenomenology of transport and in providing a theoretical framework for their description [1]. Perhaps most crucial for testing our understanding of transport is the evidence that comes from experiments in which the transient response of the plasma to thermal perturbations is studied. Different kinds of transient experiments have been performed as reviewed in [2]. Until recently, the indications coming from transient electron energy transport experiments favoured a simple linear (or weakly non linear) relation between the energy flux, q_e, and the electron temperature (T_e) gradient with a proportionality coefficient (diffusivity, defined as $\chi_e=-q_e/n_e\nabla T_e$ where n_e is the electron density) depending on local, macroscopic plasma parameters. This simple picture of **local diffusive** transport has been for the most part successful in describing the data, yet it was not clear how such a description could account for the complexity and subtleties of energy transport as unveiled by power balance studies in nearly steady state conditions.

In the past few years, a growing evidence of **nonlocal diffusive** electron energy transport has emerged from transient experiments [3-13] as discussed in [14]. The kind of nonlocality involved is limited, in the sense that a description of transport in terms of a diffusivity coefficient is still

adequate for a large class of phenomena. Nevertheless, the presence of a nonlocal component in the electron energy transport, making the diffusivity sensitive to plasma changes occurring at a distance from the measurement point, is required to explain some recent observations. The concept of nonlocality is not new in tokamak transport: a sort of nonlocal plasma behaviour was, for instance, postulated to explain the so called "profile consistency" exhibited by steady state electron temperature profiles [15] in Ohmic plasmas. Present day tokamak experiments rely generally on additional heating and improved transport regimes, but a resilience of plasma profiles to changes is still widely observed. So the evidence of nonlocal transport coming from dynamic experiments, rather than being a paradox, might actually provide the key to understand tokamak transport by bringing dynamic and steady state observations together.

A striking evidence of non local transport comes from TEXT [6, 9, 10] where a prompt temperature increase in the plasma core is observed in response to a fast cooling of the plasma edge. The experiments are based on the injection of laser ablated impurities; recently, the reverse experiment (where a sudden heating of the plasma edge causes a prompt decrease of the core temperature) has also been performed by rapidly ramping the plasma current [11]. Similar results have been reported from other tokamaks [12, 13]. In these cases the evidence generally supports the evidence of non local transport observed on TEXT. On TFTR [13] a similar phenomenology is sometimes observed, though under certain conditions the Cold Pulses (CP) following Laser Ablation (LA) propagate diffusively [16]. In JET, evidence of non local transport comes from observations of the transition from L- to H-mode confinement [3-5] [7,8]. In the transition, the diffusivity and most other transport coefficients change across the entire plasma simultaneously. More recently, studies of CP events associated with Edge Localised Modes (ELMs) have also been reported to feature non local changes in the electron diffusivity [3].

Laser ablation experiments have been proved to be a useful tool for transient transport studies for a number of reasons. The perturbing heat source (actually a heat sink) is well localised near the plasma edge. This is because the radiation comes mostly from the lower ionisation stages, which are present only at the very periphery of the plasma. Moreover, temperature and particle perturbations do not interfere: the rate of impurity particle transport has been shown to be much slower than that of heat transport and significant electron density perturbation has been found to be limited at the plasma edge [17]. Another important feature is the radial extent of the CP propagation: the T_e perturbation is detectable across the entire plasma so that limitations of other transient studies (sawtooth and pellet induced pulses) are avoided. Finally, unlike the sawtooth heat pulses, the LA CPs are not generally associated with a large scale MHD instability making the interpretation simpler; sometimes, however, an ELM instability is triggered by the LA cooling of the plasma edge and this requires some care in the analysis (see below).

In this paper an overview of Laser Ablation CP propagation experiments in JET is presented, and the results are discussed in the context of other transient transport experiments in JET and in

other tokamaks. The paper is organised as follows: in Section 2 the experimental details of LA experiments in JET and the related phenomenology are presented; Section 3 illustrates the transport analysis techniques which have been applied to these transients. The results obtained are presented in Section 4. Of particular significance are the observations of a strong non uniformity of the change in diffusivity across the plasma and an apparent relation between the strength of the plasma response to edge cooling and the plasma energy content. Section 5 is devoted to discuss the results of the present work, particularly in relation to other similar experiments; some theoretical models candidate to explain the emerging features of CP propagation in JET are also reported and discussed. Finally, some concluding remarks are summarised in Section 6.

2. EXPERIMENTAL

For the experiments reported here, the JET Laser Ablation system was used [18]. This system consists of a Q-switched ruby laser emitting a pulse of very short duration (10 ns) and energy 2-10 J. The pulse is focussed on thin (5 μm) metallic (e.g. nickel) depositions on a glass substrate. Typically much more than 10^{18} atoms are ablated in each pulse; about one quarter of the ablated atoms penetrates the plasma at high speed (about 1 km/s). The ionization length is much shorter than the width of the scrape off layer so the impurities are multiply ionised by the time they reach the plasma. Due to the intrinsic velocity spread of the particle beam, the temporal width of the impurity pulse is of the order of a few milliseconds at the plasma edge. This is still much shorter than typical particle and heat diffusive times so that the impurity source can be considered comparatively fast.

The injection of relatively large amounts of impurities affects various plasma edge parameters [14]. During the first 10-20 ms after the injection, impurity densities of up to a few 10^{16} m^{-3} are observed at the plasma edge resulting in an increase of the average ion charge (ΔZ_{eff}= 1-2). Local perturbations of the plasma electron density, n_e, are also observed with the outermost chord of the interferometer diagnostic (probing the plasma at ρ>0.9, where ρ is the geometry-independent normalised cylindrical radius) but they never exceed 10% and are normally much less than that. The increase in the total radiated power, $\Delta P_{rad,}$ revealed by bolometric measurements is very large: ΔP_{rad} values up to 20 MW have been observed, sometimes exceeding the total input power. Abel inverted bolometric signals show that the radiated power is initially (on time scales much shorter than the impurity diffusive time) concentrated outside the surface ρ=0.9. It then follows the diffusive propagation of the impurities inside the plasma. This is monitored by soft X-ray cameras which show that the penetration time for the impurities to get to ρ=0.7 is normally some tens of milliseconds; it is much faster (about 10 ms) when Laser Ablation triggers an ELM instability in H mode plasmas. As we shall see, the propagation of the Cold Pulse propagation following impurity injection is even faster, so there is no interference of

the perturbed radiated power with the CP propagation inside, say, ρ=0.8. Interestingly, once the impurities have penetrated into an H mode plasma, they diffuse away very slowly, and the radiated power can remain large for rather long times (hundreds of ms).

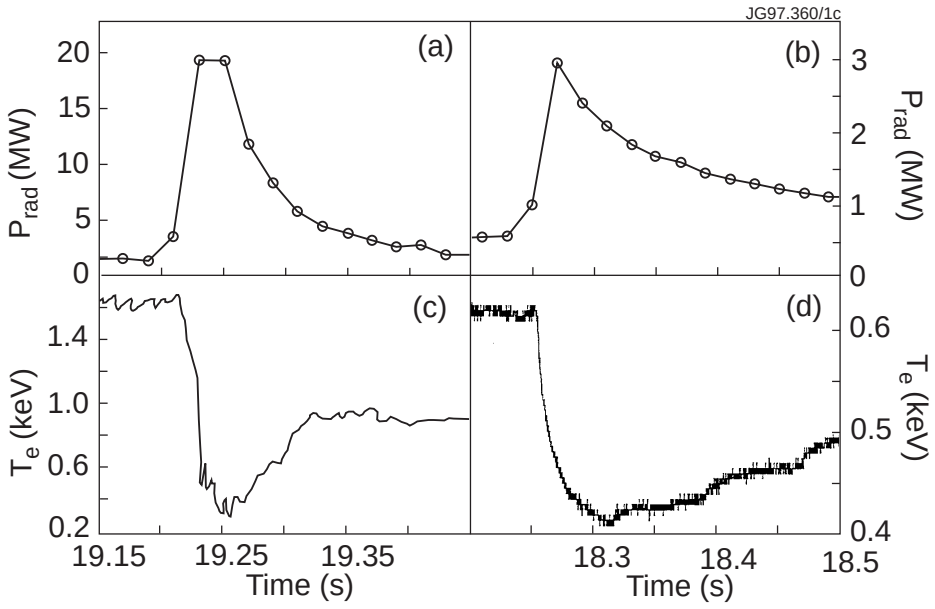

Fig.1 Time evolution of the total radiated power following Laser Ablation in JET discharges #31719 (ELMy H mode) (a) and #31376 (Ohmic mode) (b); the corresponding outermost reliable edge T_e measurements (ρ~0.8) are shown (c) (d).

Provided the increase in radiated power is sufficiently large (see below), a dramatic drop in the electron temperature, $T_{e,}$ near the edge is observed as shown in the examples of Fig.1. The T_e perturbation can be recorded by high resolution T_e measurements. On JET, these measurements are provided by a 48-channel ECE heterodyne system [19] (spatial resolution ≈ 3 cm, sampling rates up to 6 kHz, noise equivalent temperature of 10-20 eV). The diagnostic can cover the entire plasma radially on the low field side except for a gap in the ECE frequency range 73-139 GHz. Sometime it has been useful to complement these measurements with those of the 12-channel ECE polychromator which is also routinely available on JET [20]. Each diagnostic channel determines T_e at a different ECE resonance radius (R); this is converted into a normalized cylindrical radius (ρ) using the standard Lao-Hirshman representation for the JET magnetic surfaces [21].

A number of Laser Ablation Cold Pulses of this type was produced in JET plasmas and is available for analysis. Only those for which reliable heterodyne ECE measurements were available and show a distinct T_e perturbation have been analysed. This restricts the analysis to CPs produced in divertor plasmas after 1994. Most of these CPs are generated in H-mode plasmas (including Hot Ion H mode plasmas [22]), with only few pulses in Ohmic plasmas. Very recently, Laser

Ablation experiments have also been performed on JET plasmas in the so called optimised shear regime [23], but these are not reported here. The list of analysed CPs, showing the discharge number and some relevant plasma parameters, is reported in the Table.

Discharge Pulse No:	t_{LA} (s)	Mode	B_t (T)	Ip (MA)	$\langle n_e \rangle$ (10^{19} m^{-3})	<Te> (keV)	P_{NBI} (MW)	P_{rad} (MW)	ΔPrad (MW)	$\Delta P_{rad}/P_{rad}$	ELM	$\Delta T_e(0.8)$ (keV)
31329	52.2047	O	2.8	2.4	1	1.4	0	0.28	0.14	0.50		0.112
31376	58.2552	O	2.8	1.9	2	0.8	0	0.25	2.73	10.92		0.208
31768	58.0022	O	2.9	1.9	1.5	0.8	0	0.68	0.65	0.96		0.121
31769	58.0082	O	2.9	1.9	1.6	0.8	0	0.19	2.26	11.89		0.21
31774	59.0087	O	2.9	2	2	0.8	0	0.22	1.34	6.09		0.15
31327	52.2032	L	2.8	2.5	1.9	1.9	8.4	0.48	0.34	0.71		0.041
31338	51.5047	H	2.3	2.5	1.8	2.7	8.3	0.78	2.09	2.68		0.205
31341	51.5027	H	2.8	3	2.2	3.2	14.1	1.27	1.62	1.28		0.167
31342	55.8012	H	2.8	2.5	3.3	2.8	14.2	1.6	3.1	1.94		0.143
31343	55.8048	H	2.8	2.5	3.1	3.1	15.9	1.65	2.66	1.61		0.179
31344	56.2031	H	2.8	2.4	5.1	2.5	15.9	8.38	7.6	0.91		0.119
31346	56.2079	H	2.8	2.5	4.6	3.3	16	2.22	1.19	0.54		0.104
31426	56.5064	H	2.8	2.4	5.2	2.9	11.5	3.22	3.01	0.93		0.170
31719	59.2158	H ELMy	2.4	2.4	2.8	3	7	0.9	19.52	21.69		1.370
33409	52.5561	H ELMy	3.4	2.6	2.5	5.1	15.4	0.45	1.12	2.49		0.153
34475	53.3100	H Hot-ion	3.4	3.8	4	7.9	15.8	0.96	3.14	3.27	Y	–
34476	52.9112	H Hot-ion	3.4	3.8	2.8	6.6	20	0.82	2.55	3.11	Y	–
38381	52.5	H Hot-ion	2.8	2.6	1.9	3.7	16.9	0.65	0.71	1.09		0.138
38385	52.9098	H Hot-ion	2.8	2.6	2.9	5.1	16.9	0.51	2.76	5.41		0.245
38400	52.6064	H Hot-ion	2.8	2.6	2.2	3.8	15.4	0.53	1.81	3.42		0.222
38401	53.2104	H Hot-ion	2.8	2.6	3	5.1	14.7	0.66	3.88	5.88	Y	–
38683	53.0069	H Hot-ion	3.4	3	4	5.4	16.7	0.48	0.25	0.52	Y	–

Table Parameters for the JET CPs studied in this work. All values are at $t=t_{LA}$ except for ΔT_e.

Some type I ELM events, mostly triggered by Laser Ablation, are also included in the Table. It is immediately clear from the Table that all CPs analysed are associated with large increases in P_{rad}, $\Delta P_{rad}/P_{rad}>0.5$. Conversely, smaller $\Delta P_{rad}/P_{rad}$ values do not give rise to any detectable effect on ECE measurements. For $\Delta P_{rad}/P_{rad}>0.5$, the intensity ΔT_e of the T_e perturbation at $\rho=0.8$ is roughly linearly correlated with ΔP_{rad}, but with a quite large scatter in the data. Before taking this result as an evidence of a relation between the ΔP_{rad} intensity and the change in heat diffusivity following a LA, one should note that the T_e perturbation often reaches its maximum amplitude on a relatively long time scale. On such a time scale, the time evolution of P_{rad} is the dominant effect and, therefore, it influences the temperature behaviour more than the change in transport following the LA, which is expected to affect particularly the initial part of T_e drop. Other observables (see below) are therefore to be used to quantify the prompt plasma response to LA.

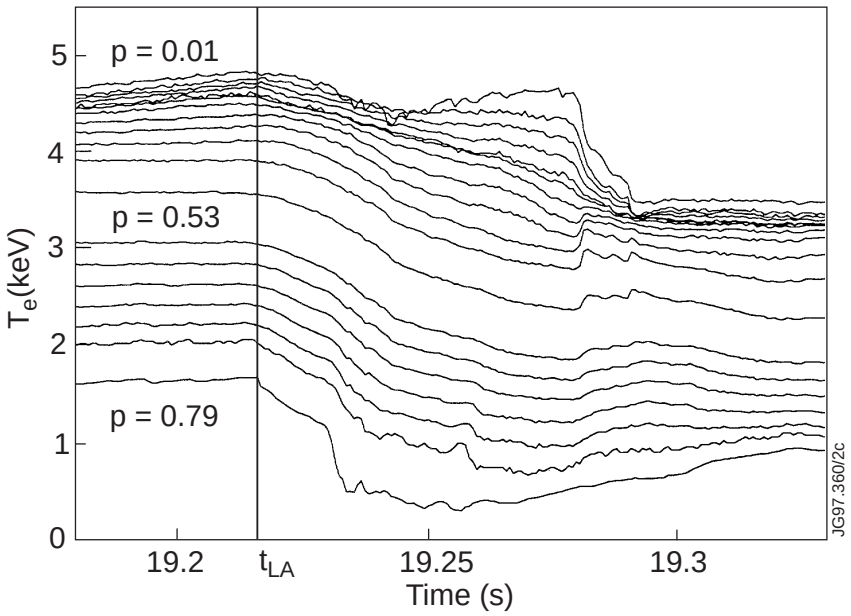

Fig.2 Time evolution of the electron temperature following Laser Ablation in JET discharge #31719. The Laser Ablation occurs at t_{LA}=19.2161 s when the plasma is in a steady state ELMy H-mode. For some ECE heterodyne channels, the normalized radius of the measurement is indicated. The sampling time was Δt=750 μs. The Cold Pulse propagates "instantaneously" from the plasma edge all the way into the plasma core. A sawtooth crash occurs at t=19.2790 s. The normalized inversion radius is ρ_{inv}=0.445.

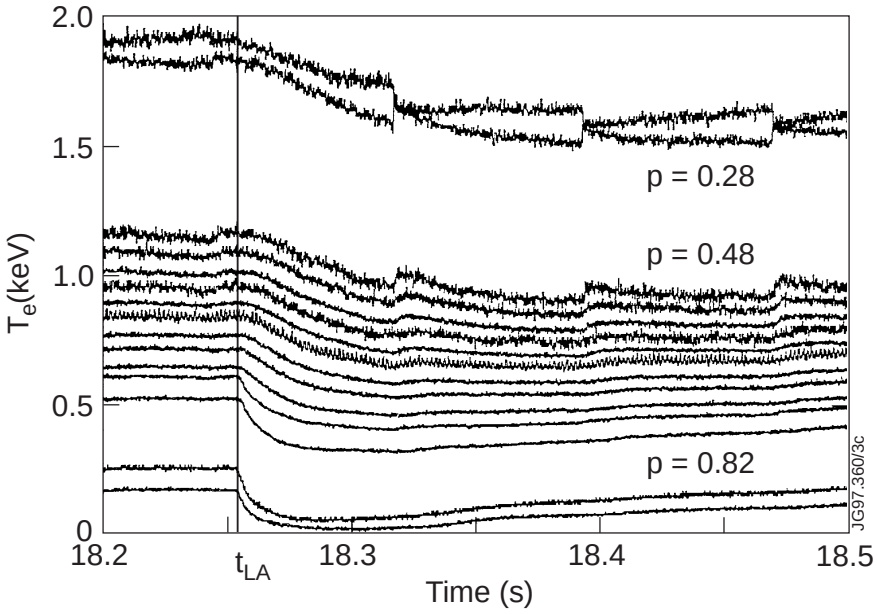

Fig 3 Time evolution of the electron temperature following Laser Ablation in JET discharge #31376. The Laser Ablation occurs at t_{LA}=18.2552 s when the plasma is in Ohmic steady state. All the available data from the ECE heterodyne diagnostic are shown. For some channels, the normalized radius of the measurement is indicated. The sampling time was Δt=170 μs. The Cold Pulse propagates inward from the plasma edge all the way into the plasma core. Sawtooth heat pulses can also be seen in the time traces riding on top of the CP, and propagating from the mixing region outwards. The normalized inversion radius is ρ=0.283.

Some CPs generated in different confinement modes are shown in Fig.2-5. Fig.2 refers to a CP in an H mode plasma. A prompt change of time derivative of T_e is observed at all radii. The T_e response is strongest near the plasma edge and within the sawtooth inversion radius (ρ_{inv}=0.44); a somewhat weaker response is observed around ρ=0.5. The exceptionally high value of $\Delta P_{rad}/P_{rad}$ is the likely cause of the very large T_e drop (ΔT_e) at $\rho \approx 0.8$.A prompt T_e response throughout the plasma is a general feature of CP propagation in all JET plasmas regardless of their mode of confinement. The example shown in Fig.3 refers to an Ohmic CP. This example of Ohmic CP is special in so far as the sawtooth activity does not prevent a useful analysis of the data inside the inversion radius. The amplitude of the T_e perturbation increases monotonically going from edge to core. Careful examination of the data shows that there is no delay of the time when T_e begins to drop in the plasma centre (ρ<0.2) relative to the T_e drop near the edge. The delay amounts to a few milliseconds around ρ=0.6. The five channels with 0.4<ρ<0.6 have a very similar time behaviour for about 50 ms following the Laser Ablation. These observations provided the first evidence of non locality of JET CPs [5].

The CPs of Fig 2-3 are somewhat exceptional in what concerns the slow recovery of T_e following the perturbation. A behaviour that is more typical of H mode plasmas is shown in Fig.4. This refers to a Hot Ion H mode. It is seen that the T_e drop is faster than in the previous cases. After a short cooling phase (lasting about 10 ms) the plasma starts to reheat from a slightly lower value of temperature, recovering on a longer time scale its regular H mode evolution.

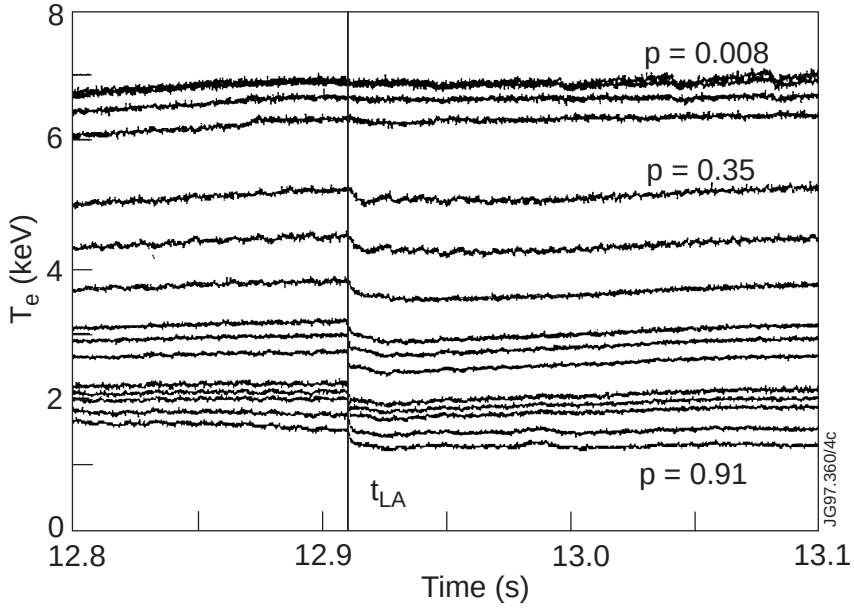

Fig.4 Time evolution of the electron temperature following Laser Ablation in JET discharge #38385. The LA occurs at t_{LA}=12.9098 s when the plasma is well into an Hot Ion H-mode.

As a final example, in Fig.5 an LA event is shown which triggered a type-I ELM instability in a Hot Ion H mode plasma. An ELM event is generally associated with an intrinsic MHD instability initiating at the very periphery of the plasma column. Hence, it is, in principle, different from a

Cold Pulse triggered by Laser Ablation, both in the cause of the event itself and in the dynamics associated with it. From the point of view of the electron temperature, however, the effect of the ELM instability is to cause an instantaneous (i.e. not resolved with a time resolution of Δt=160 μs) drop in T_e for ρ>0.7. At smaller radii, an instantaneous change in the time derivative of T_e is observed. This is similar to other Cold Pulse events and can indeed be analysed in a similar way (see below).

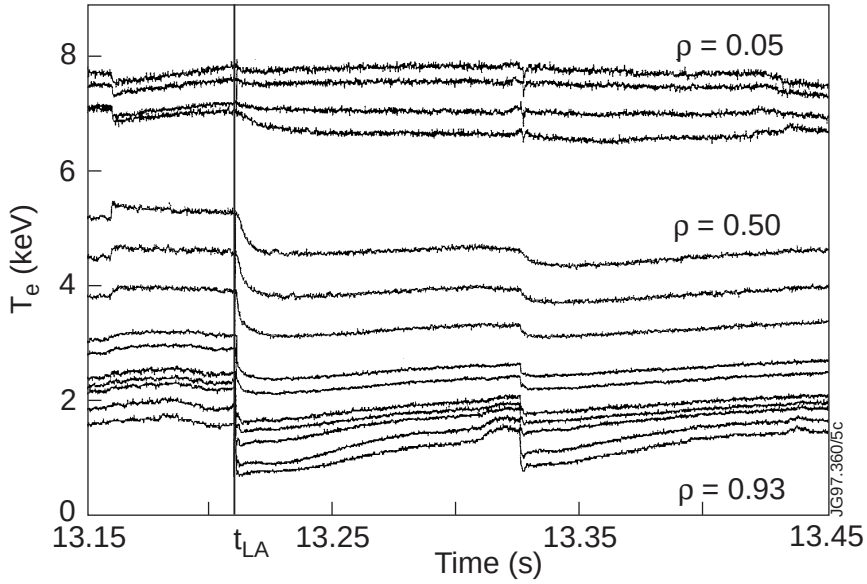

Fig.5 Time evolution of the electron temperature following Laser Ablation in JET discharge #38401. The Laser Ablation occurs at t_{LA}=12.9098 s and triggers a type-I ELM instability spoiling the Hot Ion H-mode.

3. ANALYSIS

For the analysis of CP propagation in JET three different approaches have been used. A short description of the methods of analysis used and examples of results are presented in this section.

3.1 Fourier analysis

In the Fourier method, the T_e perturbation is Fourier transformed to provide phase (φ) and amplitude (A) profiles for a number of frequencies up to a maximum set by the coherence of the signals. The applicability of the Fourier method to JET data is discussed in [24]. For the very special case of CP (inward) propagation in a region where the perturbed heat sources and sinks are negligible, the gradients of the phase (φ) and amplitude (A) for a frequency ω are approximately given by [24] $\varphi' \cong \frac{A'}{A} \cong \sqrt{\frac{3\omega}{4\chi_e^{pert}}}$ where χ_e^{pert} is the dynamic diffusivity describing the propagation of the CP. Examples of φ, A profiles for the CP of Fig.3 are shown in Fig.6. The analysis was effectively restricted to the first 20 ms of the CP by filtering the data as discussed in [24]. Four radial regions with different behaviour can be distinguished in the profiles. At radii

ρ>0.8, the effect of the heat sink is dominant. In the interval 0.6<ρ<0.8, the behaviour is similar to a simple diffusion process, and the phase and amplitude data can be reproduced with a value of χ_e^{pert}=2.5 m^2/s. At half radius (0.4<ρ<0.6), however, both phases and amplitudes are essentially independent of the plasma radius indicating non-local propagation of the CP; this is the group of five channels with identical T_e perturbation in Fig.3. Further in, the phase values decrease; this is because there is no delay in the T_e drop in the plasma centre relative to the edge.

The presence of sawtooth instabilities cannot be the cause for the sudden T_e drop in the centre. In particular, the effect of the sawtooth crash at about 13 milliseconds before the LA is to delay the central T_e drop relative to the one at half radius. So the only possible interpretation of the data is that there is a sudden increase of χ_e in the plasma core, whereas the drop at half radius is comparatively smaller. In the outer region (ρ>0.8) a sudden increase in χ_e is again required in order to explain the large drop in T_e there.

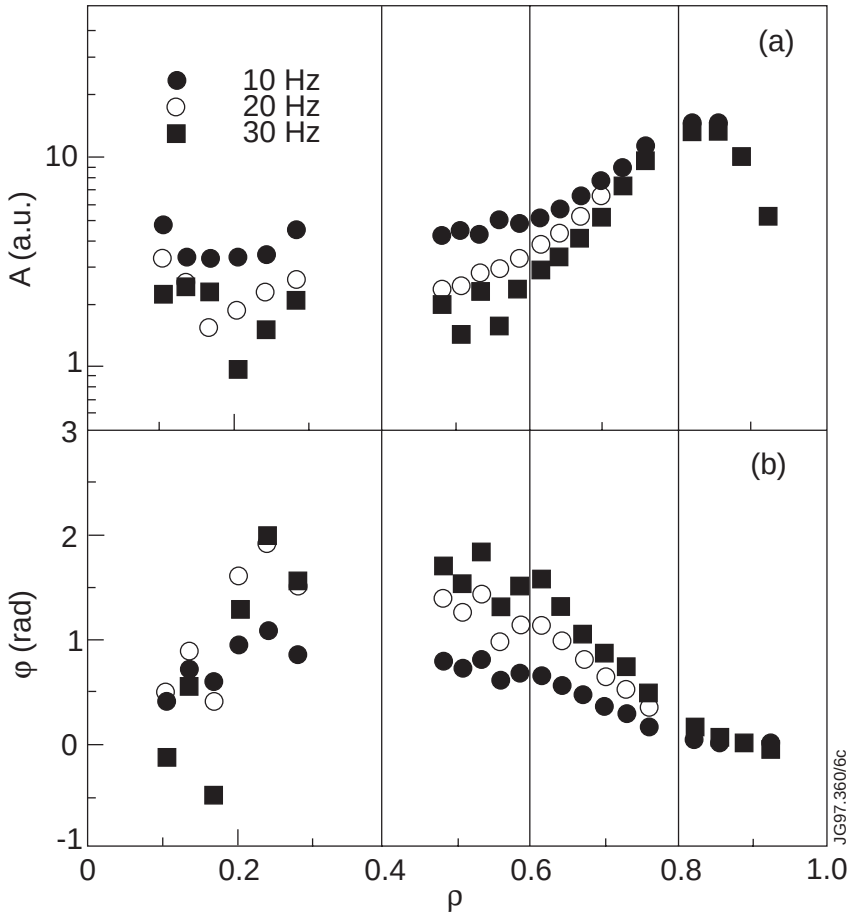

Fig.6 Fourier analysis of the CP of Fig.3. Shown are the amplitude (a) and phase (b) values for all ECE channels at the low field side. Only the frequencies where the uncertainties are smallest are shown. The bandwith, representing the effective frequency resolution of the analysis, is about 6.5 Hz. A value of the damping constant θ=20 [24] ms was used in this analysis. At values of the normalized minor radius ρ>0.77 the propagation is affected by the radiated power induced by the injected impurity. For 0.77<ρ<0.63 the profiles are consistent with a diffusive propagation with a dynamic (perturbative) electron thermal diffusivity χ_e^{pert}=2.5 m^2/s. For ρ<0.63 the propagation is much faster and exhibits a non-local character.

In most of the other Ohmic CPs, the sawtooth interference is stronger and prevents a useful analysis of the data using the Fourier technique. The Fourier analysis is of limited use in non Ohmic CPs as well. The reason is the short time scale of the change in diffusivity responsible for the observed non local behaviour in H-mode plasmas, typically about 10 ms. This explains why Fourier analysis has not been extensively used in the analysis of JET Cold Pulses.

3.2 Transport simulations

Insight into the non local character of the CP propagation and on the time scale of the change in diffusivity can be gained by simulation of the experimental T_e time traces using a transport code. The JETTO code [25] was used for this purpose in semi-predictive mode, i.e. only the heat equations are solved and the electron density profile, Z_{eff} profile, radiated power profiles, etc, are imposed throughout the computation. Also the value of the edge electron and ion temperature is imposed during the computations by using the measurements of edge temperatures available.

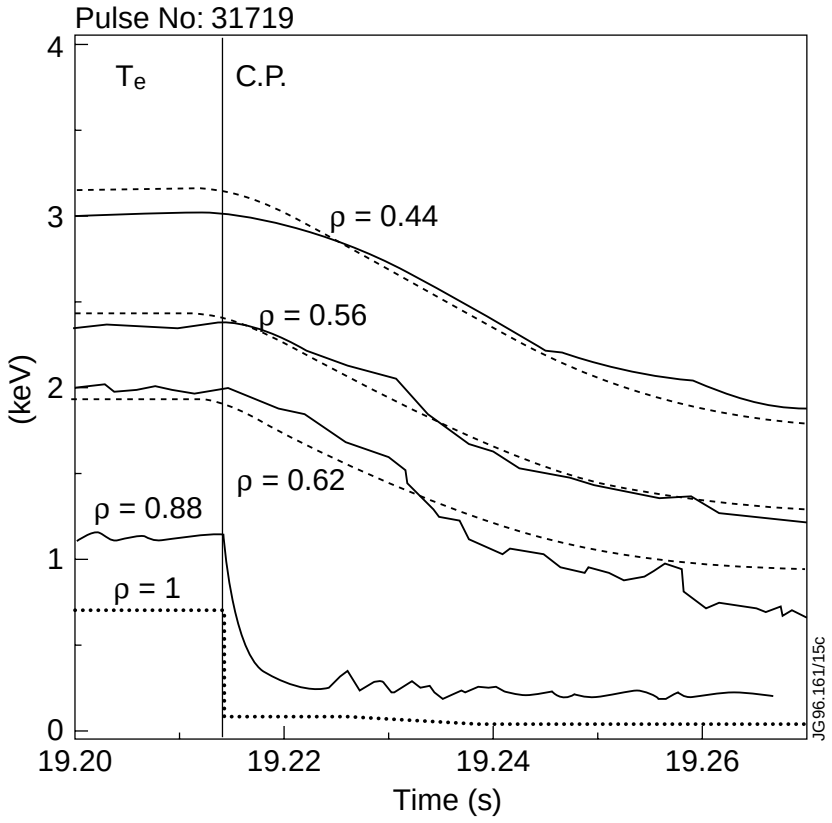

Fig.7 Comparison of the experimental (solid lines) and computed (dashed lines) electron temperature evolution at different radial positions for the CP of Fig.2. The dotted line indicates the prescribed boundary condition. Time is shifted 40 seconds back because of computational requirements.

The transport model used in the simulations is described in [26. It is based on recent theoretical work showing that the correlation length of plasma instabilities can scale as $\sqrt{a\rho_i}$ (where a is the plasma minor radius and ρ_i is the poloidal ion Larmor radius), rather than the poloidal ion

Larmor radius, due to toroidal coupling [27, 28]. The complete model is a mixed Bohm/gyro-Bohm model where a non local dependence in the diffusivity is considered in the form of a non local coefficient multiplying the Bohm like part of the diffusivity. The coefficient is given by $< \mathrm{L}^{*}_{T_e} >_{\Delta V}^{-1}$ where $\mathrm{L}^{*}_{Te}=T_e/(a\nabla T_e)$ and $<>_{\Delta V}$ means that the value is averaged over the volume $0.8<\rho<1$. This model, referred to as the L^{*}_{Te} model, has been used to simulate a number of transients in JET plasmas including L-H transitions, ELMs and Cold Pulse propagation in Ohmic and H-mode plasmas. When applied to Cold Pulse propagation, this model features an increase in diffusivity throughout the plasma when the plasma periphery is cooled by Laser Ablation. The relative change in diffusivity is not uniform, being largest where the Bohm part of the diffusivity dominates over the gyro-Bohm part, i.e. towards the plasma edge.

An example of simulation of the H mode CP of Fig.2 using the above model is shown in Fig.7. The model has been shown to reproduce most of the features of Cold Pulse propagation in JET. In particular, it is found that the explicit dependence of the diffusivity on the edge temperature gradient can generally reproduce the level of transport enhancement and its time evolution on short time scales. Some non uniformity of the diffusivity enhancement across the plasma is also predicted by the model; this, however, does not adequately reproduce the observed non uniformity (see below).

3.3 Determination of $\Delta\chi_e$ from time derivative analysis

A third method of analysis is based on the assumption that the non local effects observed are due to a sudden change of the electron thermal diffusivity, $\Delta\chi_e$, across the plasma occurring at the Laser Ablation time, t_{LA}. Under this assumption, the time derivative of T_e, $\partial_t T_e$, exhibits a discontinuity at t_{LA}, $\Delta[\partial_t T_e]_{t_{LA}} = \lim_{\varepsilon\to 0^+}\left\{[\partial_t T_e]_{t_{LA}+\varepsilon} - [\partial_t T_e]_{t_{LA}-\varepsilon}\right\}$, in proportion to the changes in the diffusivity [3]. The expression for $\Delta\chi_e$ is

$$\Delta\chi_e(\rho) = \frac{3}{2} a \frac{\int_0^\rho n_e \Delta[\partial_t T_e]_{t_{LA}} S_\rho d\rho}{n_e \nabla T_e S_\rho}$$

where a is the plasma minor radius and S_ρ is the area of the flux surface of normalised radius ρ. This expression is used here to derive $\Delta\chi_e$ from the experimentally determined density and temperature profiles.

A discontinuity in the time derivative of T_e is usually associated with a sudden change of the net heat source in the electron energy balance equation. This fact is used, for instance, to empirically determine the power deposition profile of additional heating systems such as ion or electron cyclotron heating [29]. A sudden change in χ_e gives also rise to an apparent heat source term in the equation describing the evolution of a temperature perturbation. This approach was used in [8] to determine the change in χ_e at the L-H transition in JET plasmas and is discussed more

generally in the context of the heat transients in [14] where the apparent heat source term is determined to be

$$\Delta p_\chi = \nabla \cdot \left(n_\mathrm{e} \Delta \chi_\mathrm{e} \nabla T_\mathrm{e} \right)$$

The value of Δp_χ can be estimated from $\Delta\left[\partial_\mathrm{t} T_\mathrm{e}\right]_{t_\mathrm{LA}}$ since, at $t=t_\mathrm{LA}$, energy conservation prescribes

$$\frac{3}{2} n_\mathrm{e} \Delta\left[\partial_\mathrm{t} T_\mathrm{e}\right]_{t_\mathrm{LA}} = \Delta p_\chi + \Delta p_\mathrm{rad}$$

where Δp_rad is the sudden change in radiated power density occurring at t_LA. Since Δp_rad vanishes on such a time scale for ρ<0.8, Δp_χ is simply related to $\Delta\left[\partial_\mathrm{t} T_\mathrm{e}\right]_{t_\mathrm{LA}}$. On the other hand, $\Delta\chi_\mathrm{e}$, which is directly related to transport modelling, involves a volume integral of $\Delta\left[\partial_\mathrm{t} T_\mathrm{e}\right]_{t_\mathrm{LA}}$, and is generally less accurate.

In this work, $\Delta\left[\partial_\mathrm{t} T_\mathrm{e}\right]_{t_\mathrm{LA}}$ is computed for all the CP events of the Table. Since there is nothing precluding the application of this analysis method to ELM events, these have also been analysed in the same way, taking care to exclude from the analysis the region near the plasma edge where T_e, and not just its derivative, experiences a sudden drop. In practice the change in the time derivative is determined by linear least-squares fitting of each T_e time trace over short times before and after t_LA. Fit intervals of about 4-5 ms have been used, which is a good compromise between statistical accuracy and systematic errors due to diffusion, which tend to smooth the $\Delta\left[\partial_\mathrm{t} T_\mathrm{e}\right]_{t_\mathrm{LA}}$ profile. The time scale for changes of χ_e is not much longer than 5 ms, so the $\Delta\chi_\mathrm{e}$ values obtained should be regarded as averages of some kind over the fit interval [30].

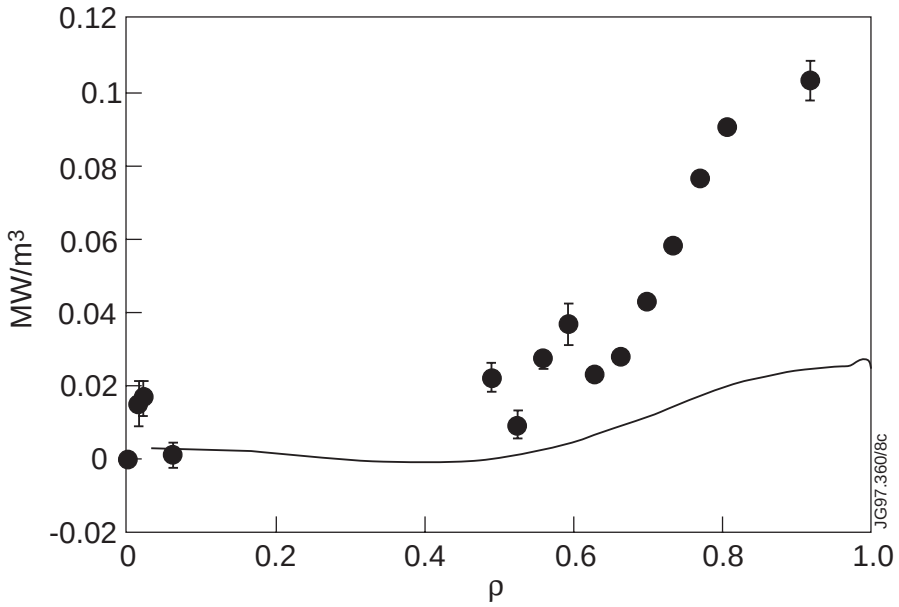

Fig.8 Comparison of $-\frac{3}{2} n_\mathrm{e} \Delta\left[\partial_\mathrm{t} T_\mathrm{e}\right]_{t_\mathrm{LA}}$ (black circles) and -Δp_rad (solid line) profiles for the H mode CP of discharge #31338. The statistical error bars of the first term, some of which are comparable to the size of the symbols, are provided by the linear least-squares fitting procedure used to calculate it.

An example of profile of the product $\frac{3}{2}n_e\Delta[\partial_t T_e]_{t_{LA}}$ for an H mode CP is shown in Fig.8. Comparison with Δp_{rad} profile shows that $\Delta p_\chi \gg \Delta p_{rad}$, i.e., the drop in the edge temperature is caused primarily by a change in diffusivity and not directly by radiation. In other words, an additional power term of the Δp_χ type must be present for at least a few ms following the Laser Ablation. In practice $\frac{3}{2}n_e\Delta[\partial_t T_e]_{t_{LA}}$ is a good estimator of Δp_χ and has been used as a measure of the plasma response to the injection of laser ablated impurities.

4. RESULTS

4.1 General features of plasma response to laser ablated impurity injection

The plasma response to Laser Ablation, as determined by the Δp_χ profile, is shown in Fig.9 and 10 for representative CP and ELM events of the Table. It is seen that Δp_χ has the same sign everywhere and affects a large plasma volume being largest towards the plasma edge. Some fine structure in the Δp_χ profile can also be seen in a few cases for ρ<0.5 and is further discussed below. There are other CP events in JET which have low $\Delta P_{rad}/P_{rad}$ values (typically $\Delta P_{rad}/P_{rad}$<0.5) resulting in T_e perturbations of too small amplitude to be distinctly identified and analysed. Although the actual diagnostic limits do not allow one to draw any firm conclusions on this point, it is believed that for these CPs the $\Delta P_{rad}/P_{rad}$ mechanism is dominant in driving temperature modifications and that, if any change in χ_e occurs, it is a very small effect. Further experimental investigation is required to clarify more in detail under which conditions and at which rate nonlocal enhancement transport effects start to become significantly dominant over the radiation trigger.

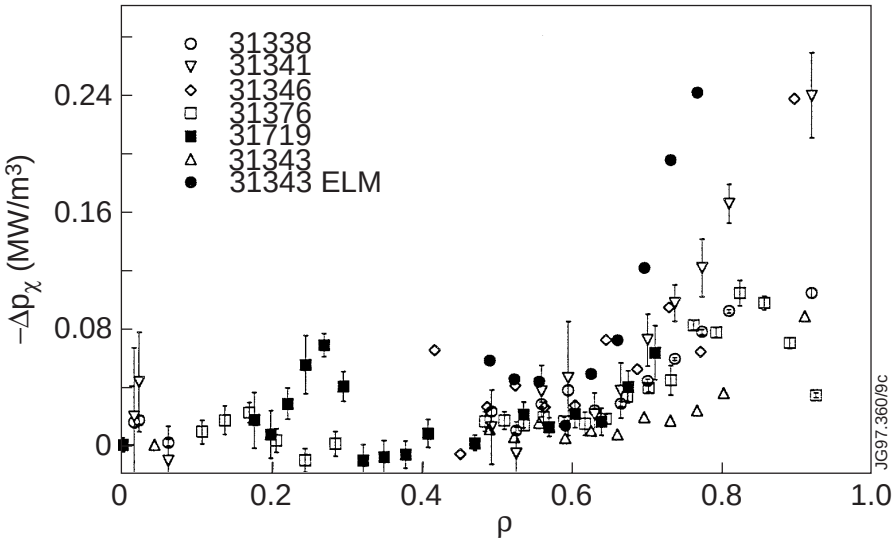

Fig.9 Spatial profiles of the perturbed heating power density -Δp_χ for Ohmic (#31376), H (#31338, #31341, #31346, #31343) and ELMy-H mode (#31719) CPs. All these CPs have moderate values of -Δp_χ . A weak -Δp_χ due to a type I ELM instability occuring in discharge #31343 is also reported.

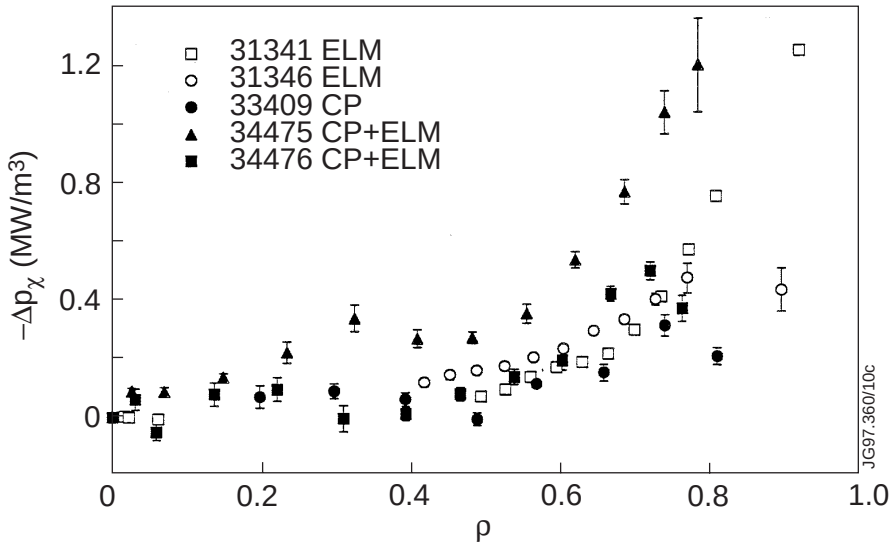

Fig.10 Same as in Fig. 9 but for stronger values ofΔp_χ. In two of these examples (#34475, #34476) Laser Ablatio triggers a type I ELM instability.

The Δp_χ profiles have been divided in two groups according to their intensity. The first group (Fig.9), has moderate Δp_χ intensities, though always much larger than the Δp_{rad} values. The value of the increase in the total radiated power, ΔP_{rad}, ranges from 0.7 to 20 MW for this group of events and is not correlated with the Δp_χ intensity. All Ohmic CPs, L and H mode CPs are included in the group of Fig.9 with the exception of one H mode CP. This (see Fig.10) has a larger intensity, comparable to that of some ELMs in Hot Ion H mode plasmas despite it was induced with a relatively weak ΔP_{rad} value (ΔP_{rad} =0.7 MW). Other type-I ELMs, on the other hand, have a weak Δp_χ like the example on Fig.9. We conclude that neither ΔP_{rad} nor the event type (CP or ELM) is responsible for the different plasma response in the two groups. Also the different time evolution of ΔP_{rad} and $\Delta\chi_e$, as indicated by transport simulations, suggests that the two quantities are not related to each other.

The combined evidence of a lower bound in $\Delta P_{rad}/P_{rad}$ for the occurrence of CP events of large amplitude (i.e. driven by a change in χ_e), on one hand, and the lack of a clear correlation between the $\Delta P_{rad}/P_{rad}$ and Δp_χ values for larger $\Delta P_{rad}/P_{rad}$ values can be explained by assuming a critical threshold mechanism in the edge temperature evolution. Above a certain $\Delta P_{rad}/P_{rad}$ threshold, the edge T_e value drops suddenly, and the ensuing changes of the gradients in the boundary plasma conditions trigger the enhanced electron energy transport in the plasma. This phenomenology is built in the L^*_{Te} model [24] by assuming the edge T_e value as a boundary condition and by incorporating a χ_e model which depends explicitly on the T_e gradient near the edge.

4.2 Relation to plasma confinement

Comparison of H-mode CPs with strong and weak Δp_χ responses suggests that Δp_χ increases when the plasma approaches the maximum energy content allowed by global stability constraints (the phase of improved confinement in JET H modes is terminated by an MHD instability destroying the conditions of improved confinement or by the so called "slow roll over" event, which practically limit the energy stored in the plasma).

To confirm this interesting observation, a dedicated experiment was performed in which the impurities were ablated at five different times in a set of similar Hot Ion H mode plasma discharges (LA time scan). In all discharges, the NBI power is increased to its maximum level at about t=52 s and kept constant for a few seconds. After a short ELMy phase lasting about 0.4 s the plasma is in an ELM free, Hot Ion H mode state of confimenent. The time evolution of T_e for two of the discharges is shown in Fig.4-5; T_e time traces at ρ=0.5 for the five discharges are shown in

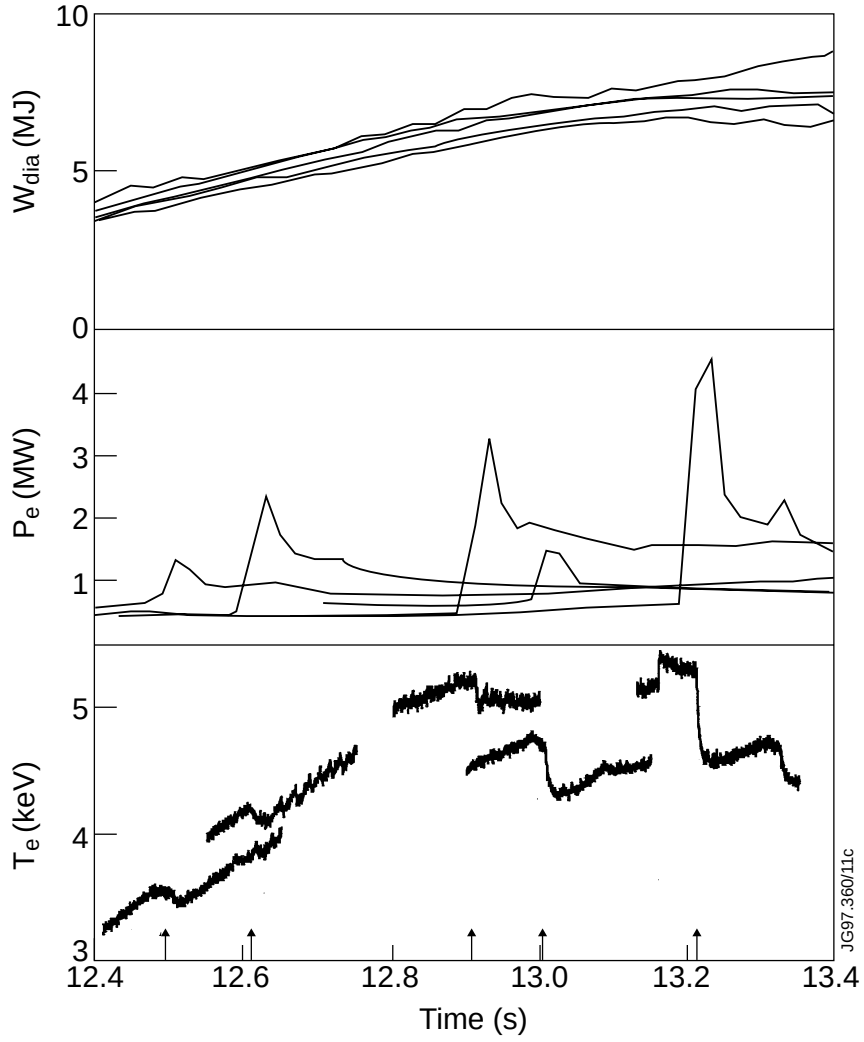

Fig.11 Time traces of the stored energy (W_{dia}), total radiated power (P_{rad}) and electron temperature (T_e) at $\rho \approx 0.5$ for five (almost identical) Hot-ion H mode discharges where the LA time was varied as shown by arrows.

Fig.11. It can be seen that the plasma response to LA is progressively stronger. This leads us to conclude that indeed a relation exists between the strength of the plasma response to edge perturbations and some unknown physical parameter related to the plasma state of attained energy confinement.

The plasma response at different times can be expressed in terms of Δp_χ profiles (Fig.12): the result is that the response is non local throughout the plasma, increases with time and is strongly non uniform.

That the intensity of the radiation is not responsible for the strength of the Δp_χ response is confirmed (see Fig.11) by the fact that $\Delta P_{rad}/P_{rad}$ is much lower for the CP at t_{LA}=53.0069 s than it is for the previous event at t_{LA}=52.9098 s, whereas Δp_χ increases monotonically with time. Incidentally, we note another interesting feature of the CP at t=52.9098 s which can be seen in Fig.13: it extends by a few hundred milliseconds the duration of the improved confinement phase, which ends at about t=53.2-53.4 s for the other shots. This is an interesting result which deserves further experimental investigation. It is tempting to draw an analogy with ELMy H-modes where steady state is achieved by periodic minor instabilities preventing the occurrence of a major instability terminating the mode. Should it be confirmed that a CP event can extend the duration of the Hot Ion H mode phase, this could be used as a means to actively preserve improved confinement for long times by external triggering of energy relaxation mechanisms.

The $\Delta\chi_e$ values determined from the Δp_χ profiles of Fig.12 are shown in Fig.14. These diffusivity enhancements are short lived: typically, after 5-10 ms the plasma starts to relax back to pre-CP conditions. In the last two cases, the LA triggers a type-I ELM instability, but only the last ELM spoils the phase of improved confinement.

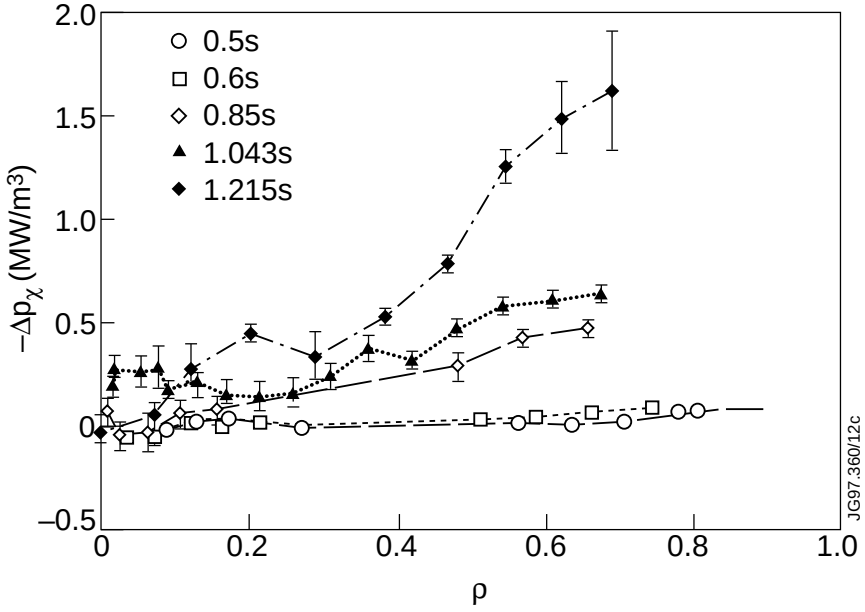

Fig.12 Spatial profiles of -Δp_χ for the five CPs of Fig.11. The time delay between the NBI switch-on time and the ablation time is reported for each discharge.

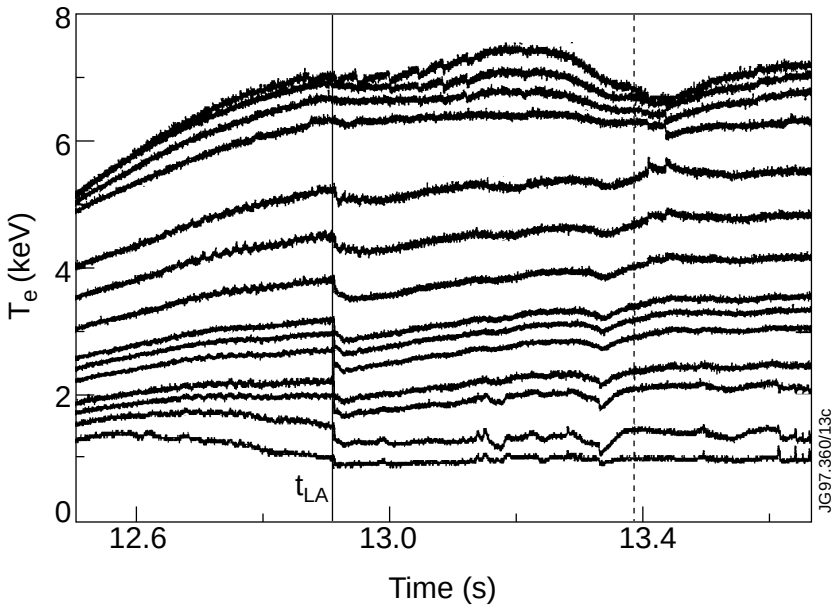

Fig.13 T_e time traces of the discharge #38385 during the good (ELM free) phase of confinement, which is exended by the impurity injection. The dashed line indicates the time limit within which the good phase of confinement of an Hot-Ion H mode discharge usually terminates. In the case it is terminated at t=53.663 s by an ELM instability.

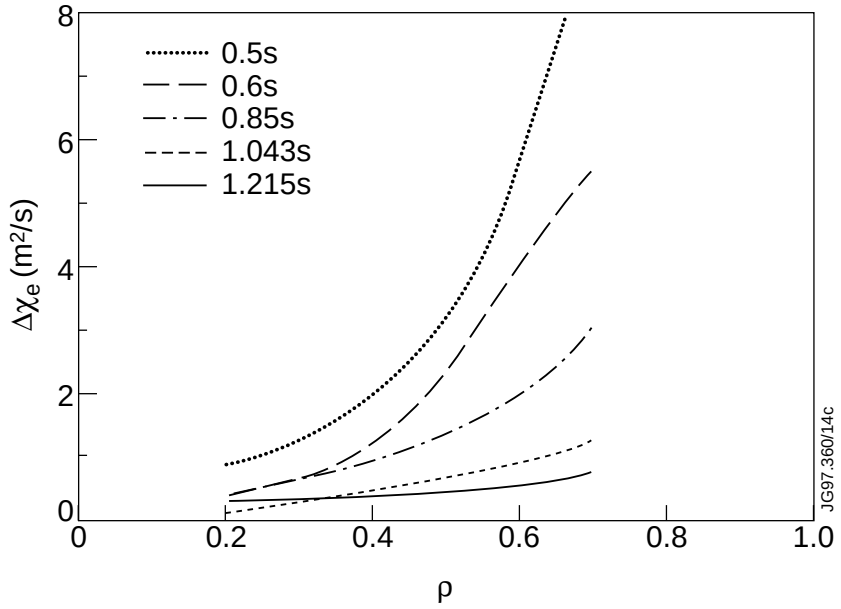

Fig.14 Profiles of the electron diffusivity enhancement $\Delta\chi_e$ following LA as determined from the Δp_χ profiles of Fig.12. Only the region where the uncertanties are not significantly large (i.e. $0.2<\rho<0.7$) is shown.

The relative variation of χ_e due to the CP is determined by dividing $\Delta\chi_e$ by the steady state diffusivity χ_e. The latter is determined from power balance simulation of a Hot Ion H mode discharge very similar to the ones of the CPs; note that the χ_e profile does not change significantly during the Hot Ion H mode phase so the same χ_e profile is used for all CPs. For the power balance simulation, the L^*_{Te} model is used. The resulting χ_e and $\Delta\chi_e/\chi_e$ values are shown in Fig.15 and 16, respectively.

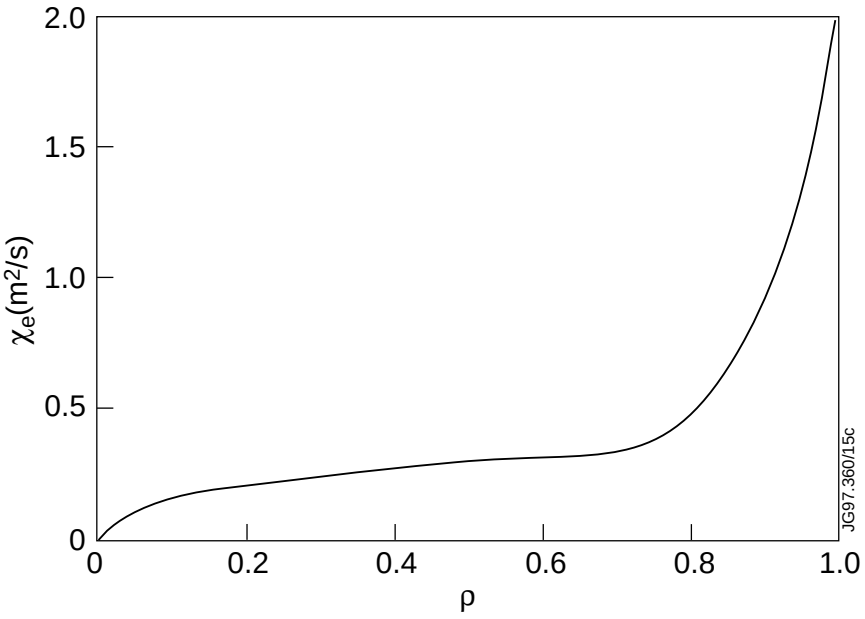

Fig.15 Steady state electron diffusivity χ_e obtained by power balance simulation of an Hot-Ion H mode discharge with same plasma parameters similar to the ones of Fig 11.

The increase of $\Delta\chi_e/\chi_e$ going from the plasma core to the edge is definitely beyond the uncertainties on $\Delta\chi_e/\chi_e$; note the log scale for the vertical axis. Like $\Delta\chi_e$, $\Delta\chi_e/\chi_e$ is an increasing function of time. Its value increases roughly exponentially with time, see Fig.17. This does not mean that a CP during the ELMy H-mode phase preceding the Hot Ion phase would have a negligibly small $\Delta\chi_e/\chi_e$ and local CP propagation. No LA was performed in this early phase, but other H-mode CPs (e.g. the one in Fig.2) show non-locality with $\Delta\chi_e \approx 1$ m^2/s, comparable to Ohmic $\Delta\chi_e$ levels (Fig. 9).

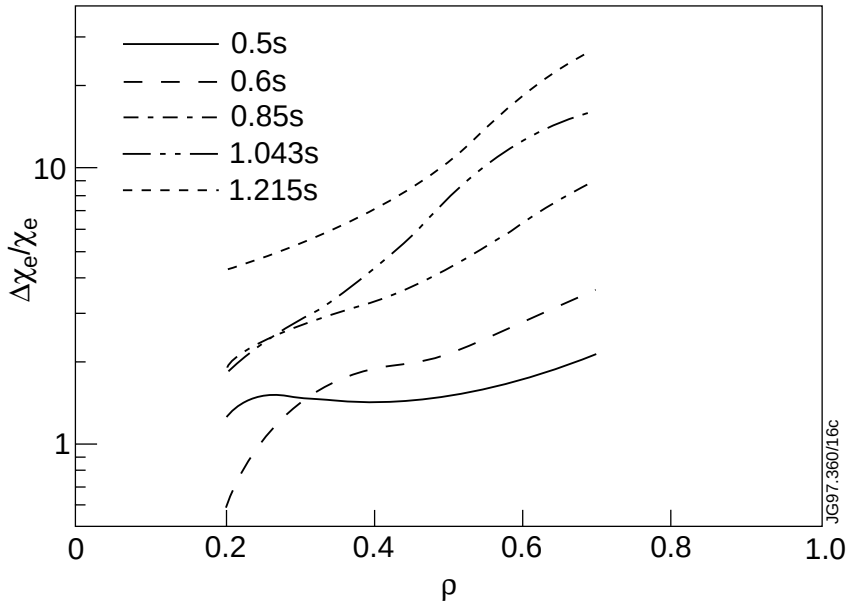

Fig.16 Relative variation of the diffusivity, $\Delta\chi_e/\chi_e$, for the five discharges of Fig 11.

4.3 Non monotonic $\Delta\chi_e$ in the plasma core

For a small number of CPs, the ECE frequency gap of the heterodyne system does not interfere with the measurement of the T_e perturbation at the low field side of the plasma. In these cases the $\Delta\chi_e$ profile can be determined reliably and fine structures modifying the exponential increase from core to edge can be looked for. In Hot Ion H mode plasmas, no fine structure is discernible

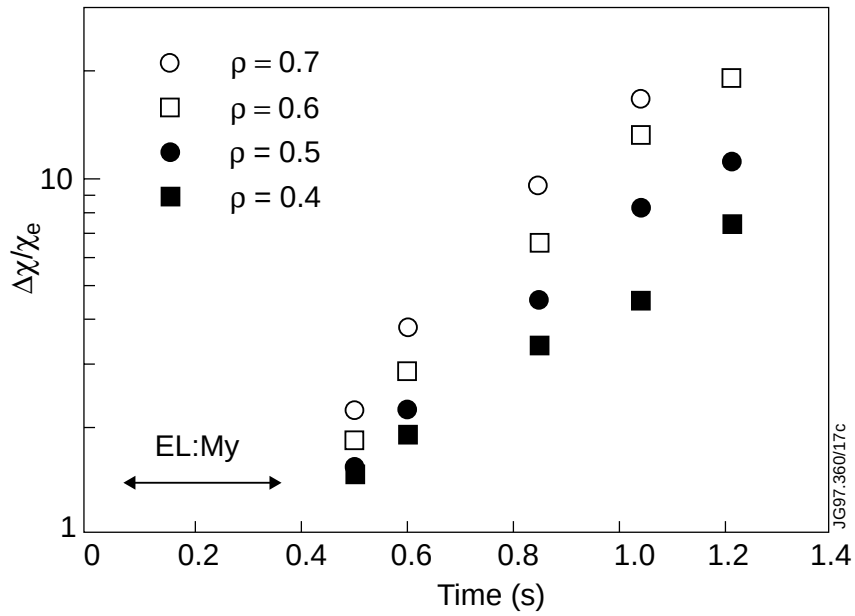

Fig.17 $\Delta\chi_e/\chi_e$ at different radii plotted versus LA time for the five discharges of Fig 11.

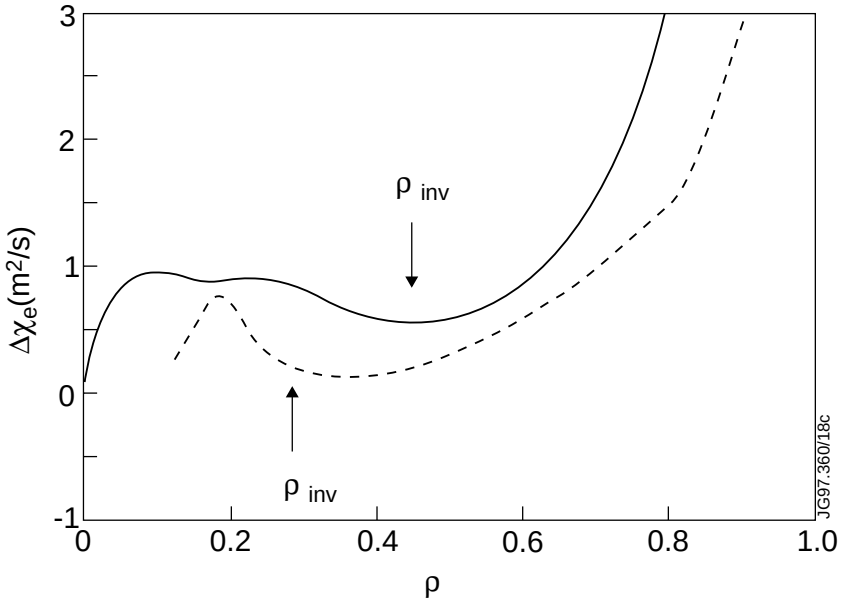

Fig.18 Radial $\Delta\chi_e$ profile for the discharges #31719 (ELMy H mode, solid line) and #31376 (Ohmic mode, dashed line). A non monotonic variation of the diffusivity is observed in these examples. The positions of the sawtooth inversion radius are also indicated.

(see Fig. 14). There are, however, two examples where a non monotonic variation of $\Delta\chi_e$ by a factor of two is indeed observed which is outside the uncertainties. The two profiles are shown in Fig.18. One is the H mode CP of Fig.2. The other is the Ohmic CP of Fig.3; actually this CP does have a gap in the data, but this does not prevent a reliable determination of $\Delta\chi_e$. $\Delta\chi_e$ is found to be of order 1 m^2/s in the plasma core; it decreases to lower values at half radius and increases strongly towards the edge. This trend reflects the trend of the Δp_χ profile and, for the Ohmic CP, the results of the Fourier analysis as well (see Fig.6).

The L^*_{Te} transport model predicts some non uniformity of $\Delta\chi_e$ of the type observed in Hot Ion H modes (monotonic increase going from core to edge), but some adjustment of the model is needed to reach a quantitative agreement between the model prediction and the observed $\Delta\chi_e$ profile. For example, the L^*_{Te} model does not predict the non monotonic behaviour of $\Delta\chi_e$ observed in the two examples of Fig.18.

Among the possible explanations for the observed oscillations of the $\Delta\chi_e$ profile a relation with the current profile can be sought. Indeed, Fig.18 shows some correlation between the location of ρ_{inv} (as determined from sawtooth crashes occurring shortly before t_{LA}) and the transition from high to low $\Delta\chi_e$ value. This evidence can be put in relationship with other studies at JET [17] indicating reduced impurity transport in L mode plasmas in the core region with low shear ($s<0.5$). The proposed explanation is that impurity diffusion is Bohm-like in the outer plasma region of high shear, whereas low shear in the plasma core decouples the Ion Temperature Gradient (ITG) microturbulence and transport becomes gyro-Bohm like. Whether the CP in certain cases destabilizes the ITG microturbulence preferentially in the plasma core and near the edge, resulting in the observed enhanced $\Delta\chi_e$ in those regions, is a question that cannot be answered at present. An alternative explanation can be sought in the form of a special role of the q=1 surface in the formation of an energy transport barrier, as observed in other tokamak experiments (e.g. RTP [31]). The experimental evidence is at present too weak to draw firm conclusions on this issue.

5. DISCUSSION

CP experiments have been performed on JET [5, 30], TEXT [6, 9, 10, 11], TFTR [13] and JIPP [12] tokamaks. The evidence from CP propagation in JET shows both similarities and differences when compared with other CP experiments. Most interesting is the comparison with TEXT CPs which were studied extensively. CP propagation is always non local in TEXT. It is also strongly non uniform, as seen in JET, but with an obvious difference: $\Delta\chi_e$ changes sign across the plasma volume being negative in the plasma core. In JET, no evidence of a negative $\Delta\chi_e$ was found in L- and H-mode plasmas; however, the non monotonic profiles of Fig.18 feature $\Delta\chi_e$ values approaching zero, if not negative, at radial positions similar to those of the negative $\Delta\chi_e$ of TEXT CPs. As for the observation of a positive $\Delta\chi_e$ in the sawtooth inversion region of JET

plasmas, it has no counterpart in TEXT, where $\Delta\chi_e$ becomes negative inside ρ_{inv}.

Further similarities and differences are found when comparing the dependence on plasma conditions of JET and TEXT CPs. Both JET and TEXT have a threshold in $\Delta P_{rad}/P_{rad}$ for the occurrence of non local CPs. The threshold is higher in JET ($\Delta P_{rad}/P_{rad}>0.5$) than in TEXT ($\Delta P_{rad}/P_{rad}>0.1$). Above this threshold, a linear relation between $\Delta P_{rad}/P_{rad}$ and $\Delta\chi_e/\chi_e$ is found on TEXT which is not found on JET. The heating and confinement regimes appear to affect some features of CP nonlocal behaviour in both tokamaks. In TEXT, the χ_e improvement in the plasma core is reduced by the application of electron cyclotron heating (ECH); in JET, the non monotonicity of the $\Delta\chi_e$ profile found in some low power discharges disappears in high power plasmas.

CP experiments on TFTR have much in common with those in TEXT. In TFTR, however, the CP propagation is found to be local in many cases, with $\Delta\chi_e^{pert}$ larger than the χ_e value from power balance analysis. A similar result is found in the Fourier analysis of the Ohmic JET CP in the region $0.6<\rho<0.8$. This result is a consequence of the low χ_e value in that region typical of low power JET discharges. A threshold in $T_e(0)/n_e(0)$ found on TFTR for the observation of non local central rise during a CP [32]. In JET the CPs are more strongly non local in good than in poor confinement discharges. A direct comparison is however not possible at the moment because no observation is addressed about the behaviour of the negative pulse on TFTR above the threshold.

The idea of non local transport was brought up long before experimental observations of the type presented here were made. Non local transport was first introduced to explain the “profile consistency” of tokamaks [15], i.e., the resilience of plasma profiles to changes that would be expected when the heating power deposition is varied inside a diffusive medium. The profile consistency is not always found in tokamaks: for instance, the same ECH off axis deposition gives very different profiles in DIII-D [33] and RTP [33]. In view of the contrasting evidence on non locality coming from steady state transport observations, transient transport experiments have been essential in providing clear evidence on the non locality of heat transport in tokamaks. A number of observations of non local transients have been made as discussed in [14]. In JET, L-H transitions [3], ELMs [4] and sawtooth heat pulses [35] have non local features, but in different degrees. There appears to be some asymmetry [36] in the inward/outward propagation: pulses involving a strong perturbation of the plasma edge (CPs, ELMs, L-H transitions) always exhibit a non local character; sawtooth heat pulses, on the other hand, can show some “ballistic” propagation but do not share the strong non locality of the other perturbations. This suggests that the plasma edge may be the source of the free energy driving the non locality of heat transport.

The observation of non locality of transport does not mean that a description of transport in terms of a diffusivity coefficient breaks down. In fact, a certain degree of linearity between

temperature gradients and heat fluxes is generally observed in tokamaks when the non local dependences of the diffusivity are kept small [37]. In this sense expressing tokamak heat transport in terms of an effective diffusivity is still a valid concept. However, one must be aware that the physical mechanisms determining the level of diffusivity of the system can have a non local character.

Several ideas have been proposed by various authors in order to explain the observed global transport modifications following a change of the plasma edge temperature. The strong coupling between edge and mid regions could be due, for instance, to plasma ability to pump up turbulence in the plasma interior due to its toroidicity [38]. This mechanism could correlate turbulence in radial direction, so that any change in the edge fluctuations would rapidly influence the transport across a large fraction of the plasma column. An alternative mechanism leading to long correlated structures is nonlinear or toroidal coupling of modes on different rational surfaces to form large radial structures. The linear theory of mode coupling, investigated for both drift waves [27] and ITG instability [28], shows eigenfunctions with a large scale length. Recent numerical simulations demonstrate that global radial structures persist even in the nonlinear regime [39].

Based on these ideas, some models have been formulated so as to reproduce, besides many features of tokamak heat transport under steady state conditions, also certain aspects of the non locality observed in transient transport experiments. The L^*_{Te} model used at JET is an example of an empirical diffusive model where non locality is built in as a dependence of the diffusivity on plasma gradients at the edge. The rationale behind this model is the idea that the free energy at the plasma edge is directly responsible for the diffusivity levels due to microturbulence with long correlation length [38]. The model can account for a number of observations, including the in/out asymmetry of transients. However the particular form of the model currently in use [26] cannot account for the strong space and time dependence of $\Delta\chi_e$ observed in Ohmic and Hot Ion H modes.

More generally, the experimental observations reported here, establishing a quantitative relation between nonlocal changes of the electron thermal diffusivity and the attained energy content (independently of the T_e perturbation amplitude), provide a basis for testing theory based transport models aimed at reproducing the salient features of tokamak heat transport under both steady state and transient conditions.

6. CONCLUSIONS

The picture of electron heat transport emerging from transient transport studies (including the Laser Ablation experiments reported here) combines local and non-local features. The non locality (or strong non linearity) required to explain the observations does not prevent a thermodynamic

description of the plasma where the electron heat flux varies in proportion to the electron temperature gradient. Another interesting feature emerging from transient transport studies is the strong non uniformity of transport across the plasma; this is by now a common observation under quasi steady state conditions, where formations of pedestals (in H mode plasmas) or transport barriers are clear examples of non uniformity.

Transient transport studies have started to unveil the complexity of tokamak plasmas. The experimental evidence accumulated so far provides some new ideas for tackling this complexity though the microscopic mechanisms responsible for tokamak energy transport are not yet understood. This type of studies provides an opportunity for detailed testing of theories of energy transport in tokamaks. It therefore ought to be pursued both in view of their relevance for the realisation of an experimental fusion reactor and for their fundamental physics implications.

ACKNOWLEDGEMENT

This work was performed under the JET-ENEA-CNR task agreement on transient transport, with financial support from JET and CNR.

REFERENCES

[1] CONNOR, J., HIDALGO, C., JACCHIA, A., ROMANELLI, F., STROTH, U., Plasma Phys. Control. Fusion **39** (1997) 609.
[2] LOPES CARDOZO, N.J., Plasma Phys. Control. Fusion **37** (1995) 799.
[3] CORDEY, J.G., et al., Plasma Phys. Control. Fusion **26** (1994) A276.
[4] PARAIL, V.V., et al., in Plasma Physics and Controlled Nuclear Fusion Research 1994 (Proc. 15th Int. Conf. Seville, 1994), Vol. 1, IAEA, Vienna (1995) 255.
[5] JET TEAM (presented by GIANNELLA, R.) in Plasma Physics and Controlled Nuclear Fusion Research 1994 (Proc. 15th Int. Conf. Seville, 1994), Vol. 1, IAEA, Vienna (1995) 51.
[6] GENTLE, K.W., et al., Phys. Rev. Lett. **74** (1995) 3620.
[7] CORDEY, J.G., et al., Nucl. Fusion **35** (1995) 101.
[8] CORDEY, J.G., et al., Nucl. Fusion **35** (1995) 505.
[9] GENTLE, K.W., et al., Phys. Plasmas **2** (1995) 2292.
[10] GENTLE, K.W., et al., The Evidence For Non-Local Transport In TEXT, submitted to Phys. Plasmas.
[11] GENTLE, K.W., et al., Bull. Am. Phys. Soc. **40** (1995) 1809.
[12] TOI, K., et al., in Plasma Physics and Controlled Nuclear Fusion Research 1996 (Proc. 16th Int. Conf. Montreal, 1996), IAEA paper CN-64/A6-5, IAEA, Vienna (1997).

[13] KISSICK, M.W., CALLEN, J.D., FREDRICKSON, E.D., JANOS, A.C., TAYLOR, G., Nucl. Fusion **36** (1996) 1691.
[14] JACCHIA, A., MANTICA, P., DE LUCA, F., GALLI, P., GORINI, G., Phys. Plasmas **2** (1995) 4589.
[15] COPPI, B., Comments Plasma Phys. Control. Fusion **5** (1980) 261.
[16] KISSICK, M.W., et al., Nucl. Fusion, **34** (1994) 349.
[17] GIANNELLA, R., et al., Nucl. Fusion **34** (1994) 1185.
[18] GIANNELLA, R., et al., Plasma Phys. Control. Fusion **34** (1992) 687.
[19] BARTLETT, D.V., et al., in Electron Cyclotron Emission and Electron Cyclotron Resonance Heating 1993 (Proc. 8th Joint Workshop Gut Ising, 1993), Max-Planck-Instituut für Plasmaphysik, Garching (1993) Vol.1, 251.
[20] BARTLETT, D.V., et al., in Electron Cyclotron Emission and Electron Cyclotron Resonance Heating 1987 (Proc. 6th Joint Workshop Oxford, 1987) Vol.?, ??.
[21] LAO, L.L., HIRSHMANN, S.P., WIELAND, R.M., Phys. Fluids **24** (1981) 1431.
[22] JET TEAM, Nucl. Fusion **32** (1992) 187.
[23] JET TEAM, in Plasma Physics and Controlled Nuclear Fusion Research 1996 (Proc. 16th Int. Conf. Montreal, 1996), IAEA paper CN-64/A5-5, IAEA, Vienna (1997).
[24] MANTICA, P., et al., Nucl. Fusion **32** (1992) 2203.
[25] CENACCHI, G., TARONI, A., JETTO — A Free-Boundary Plasma Transport Code (Basic Version), Rep. ENEA RT/TIB 88(5), ENEA, Frascati (1988).
[26] ERBA, M., CHERUBINI, A., PARAIL, V.V., SPRINGMANN, E., TARONI, A., Plasma Phys. and Control. Fusion **39** (1997) 261.
[27] CONNOR, J. W., HASTIE, R.J., TAYLOR, J.B., Proc. R. Soc. London A **365** (1979) 1.
[28] ROMANELLI, F., ZONCA, F., Phys. Fluids B **5** (1993) 4081.
[29] ROME, M., et al. Plasma Phys. and Control. Fusion **39** (1997) 117.
[30] GALLI, P., et al., in Controlled Fusion and Plasma Physics (Proc 23rd Eur. Conf. Kiev, 1996), Vol. 20C, Part I, European Physical Society, Geneva (1997) 135.
[31] HOGEWEIJ, G.M.D., et al., Nucl. Fusion **36** (1996) 535.
[32] KISSICK, M.W., CALLEN, J.D., FREDRICKSON, E.D., Further Observations Of The Nonlocal Electron Heat Transport Effect On TFTR, Rep. UW-CPTC 96-6, University of Wisconsin, Madison (1996).
[33] PETTY, C.C., LUCE, T.C., Nucl. Fusion **34** (1994) 121.
[34] HOGEWEIJ, G.M.D., et al., Phys. Rev. Lett. **36** (1996) 535.
[35] DE LUCA, F., et al., Nucl. Fusion **36** (1996) 909.
[36] PARAIL, V.V., et al., Nucl. Fusion **37** (1997) 481.
[37] BALET, B., CORDEY, J.C., Nucl. Fusion **34** (1994) 1175.
[38] KADOMTSEV, B.B., Plasma Phys. Contr. Fusion **34** (1992) 1931.
[39] KISHIMOTO, Y., TAJIMA, T., HORTON, W., LEBRUN, M.J., KIM, J.Y., Phys. Plasmas **3** (1996) 1289.